Journal Pre-proofs

Lotus-leaf-inspired non-fouling, mechanical bactericidal surfaces

Rujian Jiang, Lingwan Hao, Lingjie Song, Limei Tian, Yong Fan, Jie Zhao, Chaozong Liu, Weihua Ming, Luquan Ren

PII: S1385-8947(20)31737-X
DOI: https://doi.org/10.1016/j.cej.2020.125609
Reference: CEJ 125609

To appear in: *Chemical Engineering Journal*

Received Date: 23 February 2020
Revised Date: 20 April 2020
Accepted Date: 20 May 2020

Please cite this article as: R. Jiang, L. Hao, L. Song, L. Tian, Y. Fan, J. Zhao, C. Liu, W. Ming, L. Ren, Lotus-leaf-inspired non-fouling, mechanical bactericidal surfaces, *Chemical Engineering Journal* (2020), doi: https://doi.org/10.1016/j.cej.2020.125609

This is a PDF file of an article that has undergone enhancements after acceptance, such as the addition of a cover page and metadata, and formatting for readability, but it is not yet the definitive version of record. This version will undergo additional copyediting, typesetting and review before it is published in its final form, but we are providing this version to give early visibility of the article. Please note that, during the production process, errors may be discovered which could affect the content, and all legal disclaimers that apply to the journal pertain.

© 2020 Published by Elsevier B.V.

Lotus-leaf-inspired non-fouling, mechanical bactericidal surfaces

Rujian Jiang,[a] Lingwan Hao,[a,b] Lingjie Song,[c] Limei Tian,[*,a] Yong Fan,[b] Jie Zhao,[*,a] Chaozong Liu,[d] Weihua Ming,[e] Luquan Ren[a]

[a] Key Laboratory of Bionic Engineering, Ministry of Education, Jilin University, 130022 Changchun, China.

[b] College of Chemistry, Jilin University, 130022 Changchun, China.

[c] State Key Laboratory of Polymer Physics and Chemistry, Changchun Institute of Applied Chemistry, 130022, Changchun, China

[d] Institute of Orthopaedic and Musculoskeletal ScienceRoyal National Orthopaedic Hospital, University College London, Stanmore, HA74LP London, UK.

[e] Department of Chemistry and Biochemistry, Georgia Southern University, Statesboro, 30460 GA, USA

[*]**Corresponding author**

E-mail: lmtian@jlu.edu.cn (L.T.); jiezhao@jlu.edu.cn (J.Z.).

Journal Pre-proofs

Abstract

Antibiotics, a power tool to combat pathogenic bacterial infection, have experienced their inability to kill drug-resistant bacteria due to the development of antibiotic resistance. As an alternative, nanostructured, mechanical bactericidal surfaces may hold promise in killing bacteria without triggering antimicrobial resistance; however, accumulation of dead bacteria would greatly reduce their antimicrobial activity. In this study, for the first time we report a surprising discovery that the lotus leaf, well known for its superhydrophobicity, has demonstrated not only strong repelling effect against bacteria but also bactericidal activity *via* a cell-rupturing mechanism. Inspired by this unexpected finding, we subsequently designed and prepared a hierarchically structured surface, comprising microscale cylinders with superimposed nanoneedles on top, which was rendered superhydrophobic (water contact angle: 174 ^{o}; roll-off angle: <1 ^{o}) upon surface perfluorination. The hierarchically structured surface has displayed remarkable synergistic antimicrobial activity against *Escherichia coli*: while the majority of the bacteria (>99%) were repelled from the surface (non-fouling), those tenacious bacteria that managed to be in touch of the surface were physically killed completely. Compared to a conventional superhydrophobic surface (non-fouling to some extent, but no bacteria-killing) or a mechanical bactericidal surface (bacteria-killing but not bacteria-repelling), our new structured surface has the great advantage in maintaining long-term effectiveness in antimicrobial activity. We envisage that this study will help develop long-term effective antimicrobial strategies based entirely on physical bactericidal mechanism (thus, avoiding risks of triggering antimicrobial resistance).

Keywords: synergistic antibacterial, mechanical bactericidal, long-term antimicrobial, biomimetic hierarchical structures, lotus leaf surface

1. Introduction

The prevalence of medical-device-associated diseases caused by bacterial infections has been recognized as an extremely serious threat to global healthcare [1]. Antibiotic is one of

Journal Pre-proofs

the most important discoveries in modern medicine, but its efficacy is threatened by the evolution of resistance. Furthermore, while the resistance rate continues to rise, discovery of new antibiotics rate decreases substantially [2]. According to "the WHO Global Priority List of antibiotic-resistant bacteria developed to guide research, discovery and development of new antibiotics", developing new antibiotics are top priority tasks to fill the gap between the urgently needed treatment of anti-infection and the rise of drug-resisitance [3,4]. As an alternative, natural or bio-inspired surfaces covered with dense nanoscale pillars, demonstrating remarkable bactericidal performances [5-13], have been considered as a promising way to combat the emerging worldwide epidemic of bacterial resistance to antibiotics [14-16]. Differing to conventional bactericides, those nanostructured surfaces can physically kill adhered microorganisms *via* mechanical rapture of bacterial cells by nano-pillar arrays without triggering any potential antimicrobial resistance (AMR) [17-21]. Nevertheless, the lethality of the nano-pillar arrays can be largely compromised or even deprived due to the accumulated dead bacteria and debris, which may even serve as nutrients in the subsequent bacterial proliferation [22,23]. Consequently, it is hard to obtain a long-term antibacterial surface only relying on the mechano-killing capability.

Alternatively, lotus leaf surface, as one of the most famous superhydrophobic surfaces, displays excellent anti-biofouling performances, primarily ascribing to the stable air cushion entrapped at liquid/solid interfaces, which significantly reduces the contacting area and minimizes the biofouling [24-31]. However, once attached, microorganisms are hard to be inactivated since the bactericidal nature is lacked on superhydrophobic surfaces [32-36]. Hence the following bacterial proliferation and colonization are inevitable. Far different from the previous notion about the sole anti-biofouling performance of the lotus leaf [25,37], in this research, we unprecedentedly discover that natural lotus leaves not only possess super-repellency towards microorganism, but also demonstrate inherent bactericidal activity against the adhered bacteria. In light of the lotus leaf structures consist of micro-sized papillae and

nano-sized outermost wax tubes with similar aspect ratio to the bactericidal nanopillars [6,28], we envisage that the bactericidal activity of this superhydrophobic surface might result from the mechanical killing mechanism.

Herein, we investigate the super-repellency (the non-fouling property) of the lotus leaf towards the bacterial medium, together with its mechanical bactericidal activity against the attached bacteria, and for the first time reveal the synergistic antibacterial effects of its bacterial repellency and physical rupture by nanotubes. Inspired by this, a hierarchically structured superhydrophobic surface integrated with regularly spaced micro-pillar arrays and packed nanoneedles is designed and developed, which exhibits remarkably antibacterial performances against *Escherichia coli* (*E. coli*) at a high concentration (10^8 CFU mL^{-1}) under a prolonged incubation time. Compared with conventional antibacterial strategies, the as-prepared samples maintain high-efficiency antibacterial performances through the combination of super-repellent property and mechanical sterilization, all of which arise from the physical phenomena. Notably, the arrangement of the nano-structures of lotus leaf surface is different from previous mechanical bactericidal structures which are usually vertically arranged, accordingly, this work may provide a deeper understanding about mechanical bactericidal structures.

2. Experimental Section

2.1 Miro-cylinders were fabricated on silicon (100) wafers

The micro-patterns were defined onto a photoresist (AZ524) by standard an UV-lithography step. To construct a masking layer for the subsequent etching process, the 1 μm silicon oxide layer was coated on the place not covered by the photoresist. Thereafter, miro-cylinders were fabricated by alternating cycles of passivation with C_4F_8 (C_4F_8 flow 190 sccm) and reactive ion etching with SF_6 (SF_6 flow 450 sccm). The etch rate was measured to be 5 μm min^{-1} [39-41].

2.2 Growing ZnO nanoneedles on substrates

The NaOH solution in methanol (0.03 M) was added slowly to a solution of zinc acetate (0.01 M) in methanol and stirred at 60 °C for two hours and a clear homogeneous solution was obtained. The resulting transparent solution is stable enough for keeping in 4 °C freezer at least two weeks. The synthesized ZnO nanocrystals were spin-cast (at 3000 rpm for 20 s) four times onto the clear substrates (flat silicon and micro-structured silicon) to form a thick film of crystal seeds. After every spin-casting, the substrates were annealed at 400 °C for at least 30 min. After uniformly coated with ZnO crystal seeds, a modified hydrothermal method was used to grow ZnO nanoneedles on substrates. The seeded substrates were immersed upside-down in an open crystallizing dish containing an aqueous solution of 4 M zinc nitrate hexahydrate and 4 M sodium hydroxide at 60 °C for 80 min. The substrates were then removed from solution, rinsed thoroughly with deionized water, and dried [42].

2.3 Surface hydrophobization

To obtain low surfaces energy similar to that of lotus leaves' epicuticular waxes, all the structured substrates were immersed in the 2.0 wt.% ethanol solution of trimethoxy(1H,1H,2H,2H-heptadecafluorodecyl)silane for 2 h at room temperature and then taken out to heat at 80 °C for 1 h [42].

2.4 Antimicrobial tests of lotus leaves:

The obtained fresh lotus leaves were cut into pieces 1 cm by 1cm in size and attached to a 1 × 1 cm^2 polyethylene terephthalate (PET) film as flatly as possible. The flat lotus leaves were cleaned with ultrapure water for three times. Then the cleaned lotus leaves were immobilized on the bottom of 12-well plates and covered with 2 mL bacterial solution (10^8 CFU mL^{-1}). Lotus leaves were co-cultured with bacteria for different time intervals (3, 6, 12, and 24 h, respectively) at 37 °C, and fresh bacterial suspension was changed every 6 h for the long-term incubation. After incubation, the bacterial suspension was removed and the lotus leaves were gently taken out then washed with sterile PBS for three times. To evaluate the number and morphology of the adhered bacteria, the cultured lotus leaves were immobilized by 4%

paraformaldehyde for 60 min and washed with sterile PBS for three times. After freeze-drying, the lotus leaves were investigated by using field emitted scanning electron microscopy (SEM, XL 30 ESEM FEG, FEI Company, USA). Confocal laser scanning microscopy (CLSM; LSM 700, Carl Zeiss) was employed to assess the viability of adhered bacteria on the lotus leaves. Before observation, the sample was stained by LIVE/DEAD BacLight Bacterial Viability Kit for 15 min in dark and gently washed with sterile PBS for three times subsequently undergoing a freeze-drying procedure. Viable (appearing green) and dead (appearing red) bacterial cells can be easily distinguished with fluorescent microscopy. The percentage of the occupied area of adherent bacteria from the fluorescent images were counted using ImageJ software. As references, the pristine silicon wafer and the gold-film coated lotus leaves were conducted under same conditions.

2.5 Inhibitory zone test of the lotus leaf

The bacterial suspension (100 μL, 10^6 CFU mL^{-1}) was spread uniformly on a LB-agar plate. A fresh lotus leaf attached on the PET film was placed upside-down on the center of an agar plate and incubated for 18 h at 37 °C. The inhibition zone was visualized and recorded using a digital camera

2.6 Antimicrobial tests of artificial structures

These procedures are performed similarly to that of lotus leaves and more details can be seen in the supporting information.

3. Results and discussion

3.1. Lotus leaf surface characterizations

Fully developed lotus (*Nelumbo nucifera*) leaves (Changchun, Jilin, China, 43° N, 125° E) were collected to investigate their antibacterial behaviors. **Fig. 1a** shows the typical digital photographs of the local lotus leaf and an almost ball-shaped water droplet on this non-wettable surface. As shown in **Fig. 1b-d**, the leaf surface is featured with hierarchical structures composed of micro-sized protrusions (~5-10 μm in diameter) and nano-sized wax

Journal Pre-proofs

tubules (~0.3-1.1 μm in length and ~0.1-0.2 μm in diameter). The superimposed nanoscale layer (**Fig. 1d**) built by the three-dimensional wax tubules of high aspect ratio is much similar to the bactericidal surfaces of dragonfly and cicada wings [6,7]. By combining the hierarchical structures with the low-surface-energy wax, a superhydrophobic surface with a high static contact angle (CA = 154° ± 5°) and an ultralow roll-off angle (RA = 5° ± 2°) can be obtained (**Fig. 1e**), which is responsible for the extraordinary super-repellent property of lotus leaves [24,37].

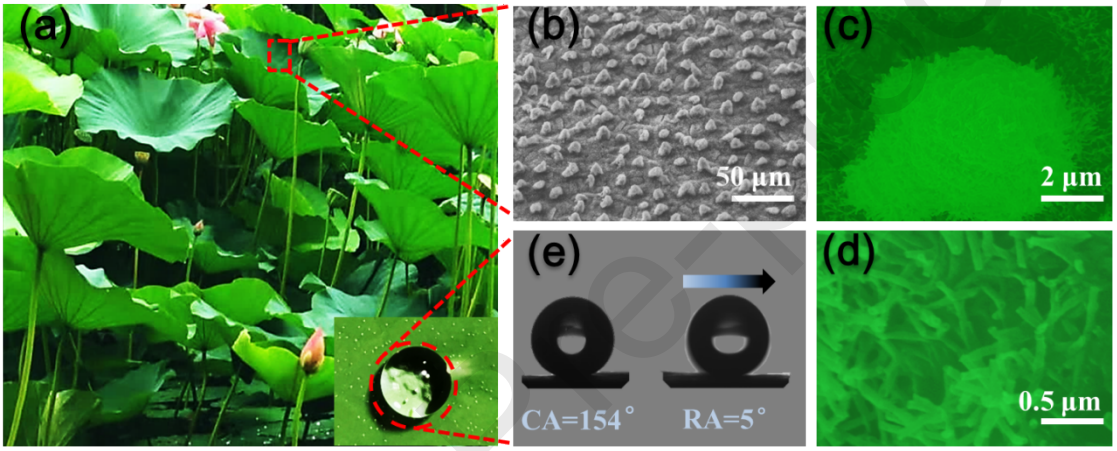

Fig. 1. Images of the lotus leaf and water droplet on the surface. (a) Typical digital photographs of superhydrophobic lotus leaves and the water droplet on the lotus leaf. (b) SEM image of the lotus leaf tilted at an angle of 45°. (c,d) Magnified SEM images of a single papilla (c) and nanotubes (d). (e) The CA and RA of the lotus leaf.

3.2 Lotus leaf surface antibacterial properties

Gram-negative *E. coli* was chosen as the representative microorganism to explore the bacterial repellency and bactericidal properties. Briefly, selected lotus leaves (1 × 1 cm^2) were immersed in 2 mL suspensions of *E.coli* (~10^8 CFU mL^{-1}, phosphate buffered solution (PBS)) for different time intervals (3, 6, 12, and 24 h respectively). The suspension was replaced every 6 h to maintain the bacterial cell vitality for the long-term incubation. The adhered bacteria on the samples were freeze-dried, gold-coated and imaged by scanning electron microscopy (SEM). To further confirm bacteria states, the samples were viewed under the

confocal laser scanning microscopy (CLSM) after being stained with a LIVE/DEAD Baclight Bacterial Viability Kit (L-7012) (Viable or dead cells can be stained as green or red respectively). As shown in **Fig. 2**, compared to the blank silicon wafer, lotus leaf surfaces exhibit significantly lower level of bacterial adhesion over all the incubation periods. Particularly, almost no bacterium is found on the lotus leaf surface after the initial 3 h incubation, revealing the excellent anti-adhesion activity which mainly due to its super-repellency (non-fouling property) against the bacterial medium. A time-related increase of the bacterial adhesion on the superhydrophobic leaf surface is observed through a quantitative calculation of the bacterial coverage by CLSM **(Fig. S1)**. Up to 19-fold increase in the number of attached bacteria is observed on the samples after 24 h incubation as compared to that with 3 h incubation. This result evidently indicates that the air cushion entrapped at solid/liquid interfaces plays an essential role in impeding bacterial adhesion at the initial stage, but may gradually lose its efficiency because of the impairment of air cushion with the prolonged immersion time [38].

Whereas, as shown in **Fig. 2a and S1**, it is worthing to mention that nearly all of the cells adhered on the lotus leaf are dead (stained in red) during the full observation periods in the range from 3 to 24 h, clearly indicating the inherent bactericidal property of the leaf surface. To further explore the bactericidal mechanism, morphologies of attached bacterial cells were evaluated by SEM images. As illustrated in **Fig. 2b,c**, compared to the intact cells on the planar silicon, the adhered bacteria on lotus leaves are highly deformed and the cellular components are engulfed by the spaces between nanotubes. Indeed, these results are very similar to those on dragonfly or cicada wings [5,10], confirming our hypothesis that the bacterial inactivation on the lotus leaf surface originates from the mechanical rupture of the cells by the densely assembled nanotubes with the high aspect ratio. Notablely, the bacterial cell walls are engulfed into the spaces of randomly oriented nanotubes instead of merely devoured by the vertically arranged nanotubes (**Fig. 2b**). In other words, this is a powerful

evidence that the nanotubes stretch the cells membrane rather than piercing the membrane through its sharp tips, finally resulting in the death of attached bacteria.

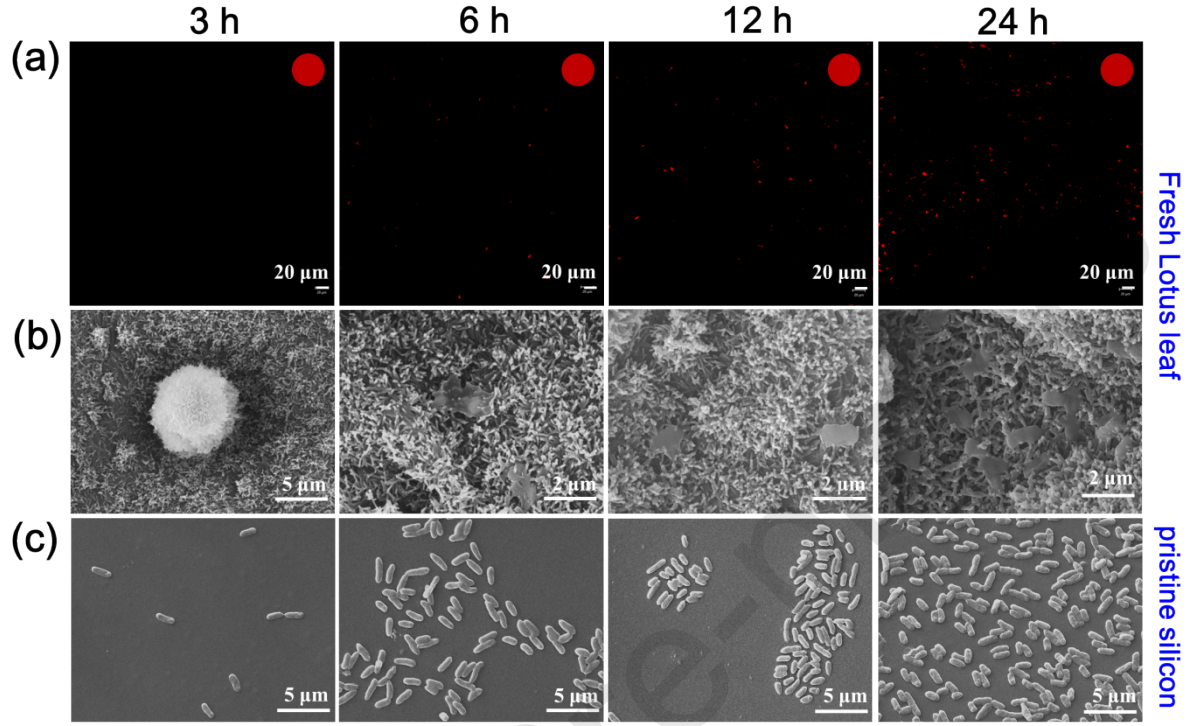

Fig. 2. Representative SEM and CLSM images of bacteria on the pristine silicon and fresh lotus leaf surfaces after 3 h, 6 h, 12 h and 24 h incubation. (a) CLSM images of *E. coli* cells attached on lotus leaves and insets in the top right corner present the percentages of live bacteria (green) and dead bacteria (red). (b) SEM images of *E. coli* cells morphologies on fresh lotus leaf surfaces. (c) SEM images of *E. coli* cells on the flat control silicon surfaces.

To gain insight into the proposed bactericidal mechanism, lotus leaves were coated with a non-toxic gold-layer (~10 nm) to eliminate the influence of the surface chemistry on bactericidal activity. As shown in **Fig. 3a,b,** similar to the pristine lotus leaves, the *E. coli* cells on the lotus leaves coated with gold-film are obviously altered the morphologies. CLSM images confirm that *E. coli* cells attached on lotus leaves coated with gold-film are nonviable (**Fig. 3c,d**). Moreover, zone of inhibition assay was performed to determine whether the leaked chemical components of the lotus leaf account for the death of bacteria. As shown in **Fig. 3e**, no inhibition zone is found around the lotus leaf, demonstrating that the disengaged

chemical components are not responsible for the bacteria death. Additionally, the yellow constituents that surround the lotus leaf from itself can be observed and show any adverse effect on the contacted bacteria. These results together confirm that both the super-repellency and bactericidal property of the lotus leaf originate from its structures. Notably, considering the random arrangement of the nanotubes on the surface which is different from usually vertically arranged bactericidal structures, this finding may provide a deeper understanding about mechanical bactericidal structures.

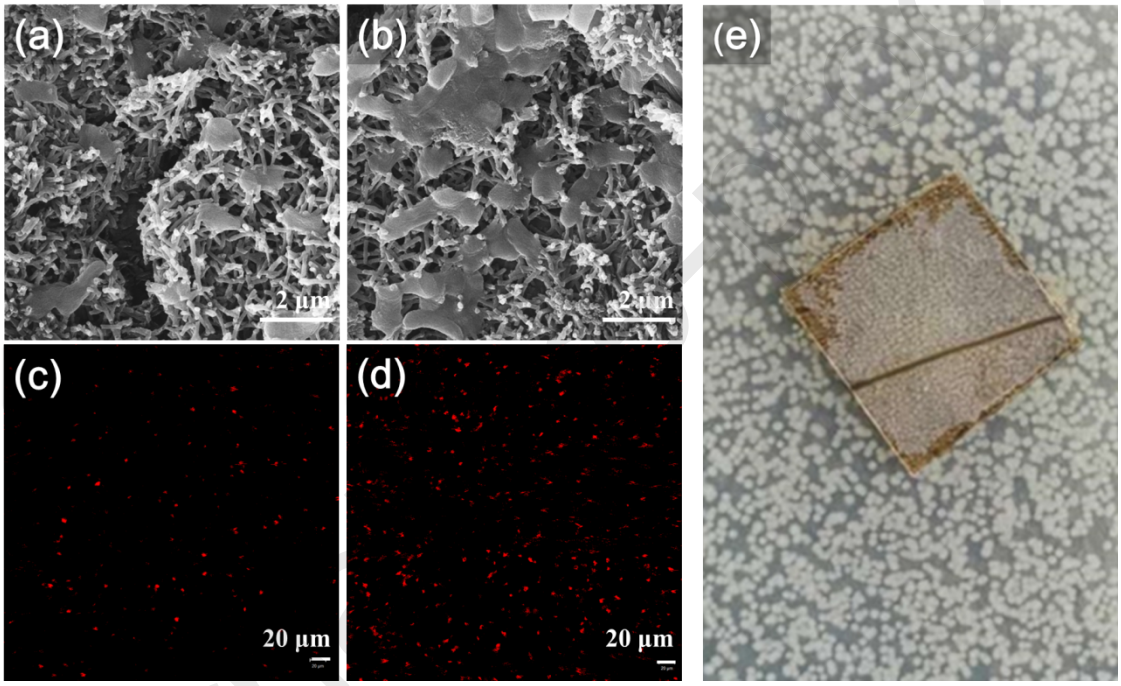

Fig. 3. Representative SEM images of *E. coli* cells morphologies attached on lotus leaves coated with gold-film after 3 h (a) and 24 h (b) incubation. CLSM images of bacteria on the gold-film coated lotus leaf surfaces after 3 h (c) and 24 h (d) incubation. (e) Digital images of the inhibition zones of lotus leaf against *E. coli*.

3.3 Biomimetic surfaces fabrications and characterizations

Inspired by this synergistic antibacterial effect of lotus leaf, an extended effective antibacterial surface endowed with both excellent bacterial super-repellency (non-fouling property) and mechanical bactericidal performance has been designed and developed, which can remarkably prolong its efficiency under much harsh conditions with respect to the

conventional superhydrophobic surfaces, without causing any potential AMR. Briefly, a hierarchical surface with both micro-scale cylinders and nano-scale needles was fabricated *via* a combination of plasma etching and hydrothermal reaction **(Scheme 1)**. The vertically aligned silicon miro-cylinders (~5 μm in diameter, ~13 μm in height and ~12 μm in interval) were readily manufactured through a plasma etching strategy **(Fig. 4a,b and S2a,b)** [39-41]. This micro-scale cylinders patterned silicon wafer is denoted as MS according to its surface structures. Subsequently, zinc oxide (ZnO) nanoneedles, acting as the nanotube analogues of lotus leaves, were delicately constructed on the MS surface *via* a low-temperature (60 °C) hydrothermal approach [42]. Similar to the lotus leaf, the prepared surfaces evidently display the hierarchical structures, consisting of the micro-scale cylinders and the nano-scale ZnO needles **(Fig. 4c,d and S2e-h)**. This dual-scale structured surface is nominated as DS. Flat silicon wafer was directly covered with ZnO nano-scale needles to get the single-scale structured sample and marked as NS. As displayed in **Fig. 4e,f** and **S2c,d**, the diameter of the nanoneedle tip is ~30-50 nm with average height of ~2-2.5 μm, presenting a high aspect ratio which is comparable to the reported structures with excellent mechanical bactericidal performances [17,43].

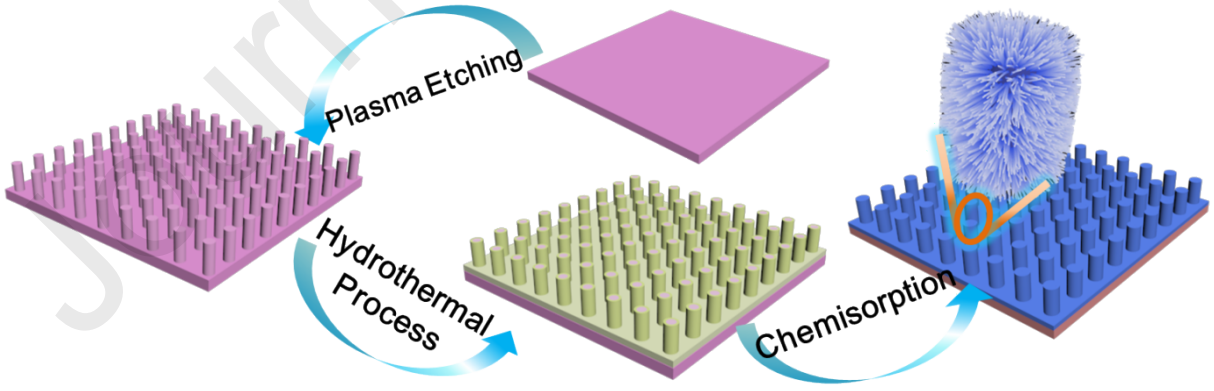

Scheme 1. Schematic illustration of fabrication procedure of lotus leaf-like structures.

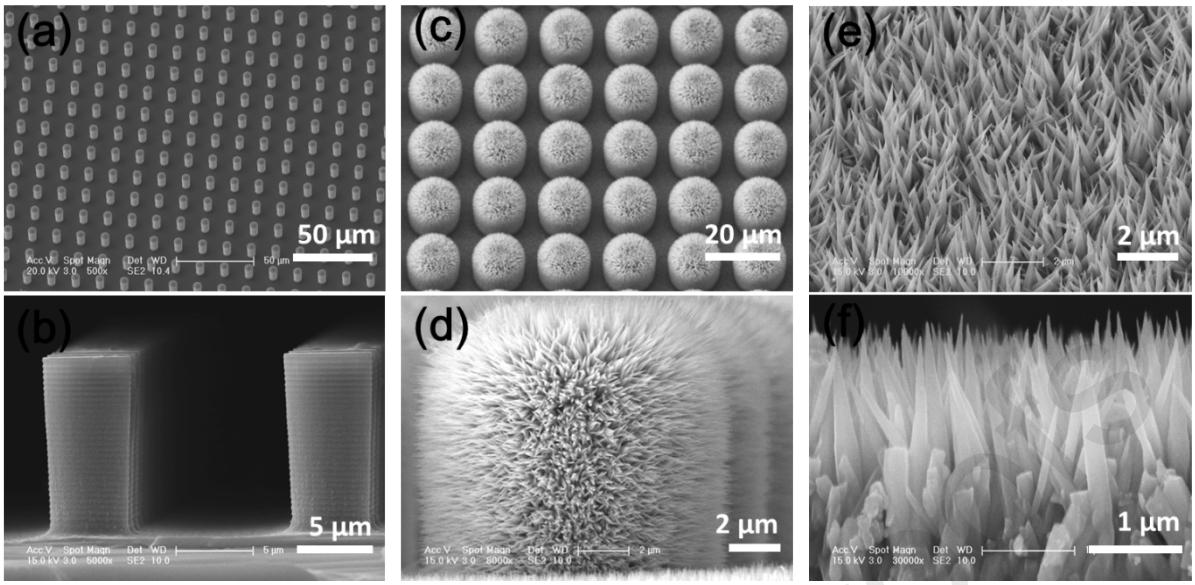

Fig. 4. SEM images of microscale structure patterned silicon surface (MS) (a) and (b), dual-scale structures patterned surface (DS) (c) and (d), and pure nanoscale structure patterned surface (NS) (e) and (f), tilted at an angle of 45° ((a), (c) and (e)), or at cross-sectional views ((b), (d) and (f)).

To render these structures low surface energy, all the samples (NS, MS and DS) were treated with fluoroalkylsilane through a chemisorption process, which were denoted as NSF, MSF and DSF, respectively. Energy dispersive X-ray spectroscopy (EDS) in SEM and X-ray photoelectron spectroscopy (XPS) were employed to elucidate the surface chemistry after modifications. As shown in **Fig. 5**, compared with untreated NS and DS, there are three new peaks (C-O (~287 eV), CF_2 (~292 eV), and CF_3 (~294 eV)) appear on the corresponding fluorinated samples (NSF and DSF), indicating the fluorinated surfaces are successfully modified with hydrophobic chemical groups. In addition, as displayed by the elemental mapping **(Fig. 6a-c and S3)**, fluorine element (marked green color**)** is homogeneously distributed on all the fluorinated surfaces. Thus, as exhibited in **Fig. 6c**, the hierarchically structured superhydrophobic surface, as a counterpart of lotus leaf surface, is completely fabricated.

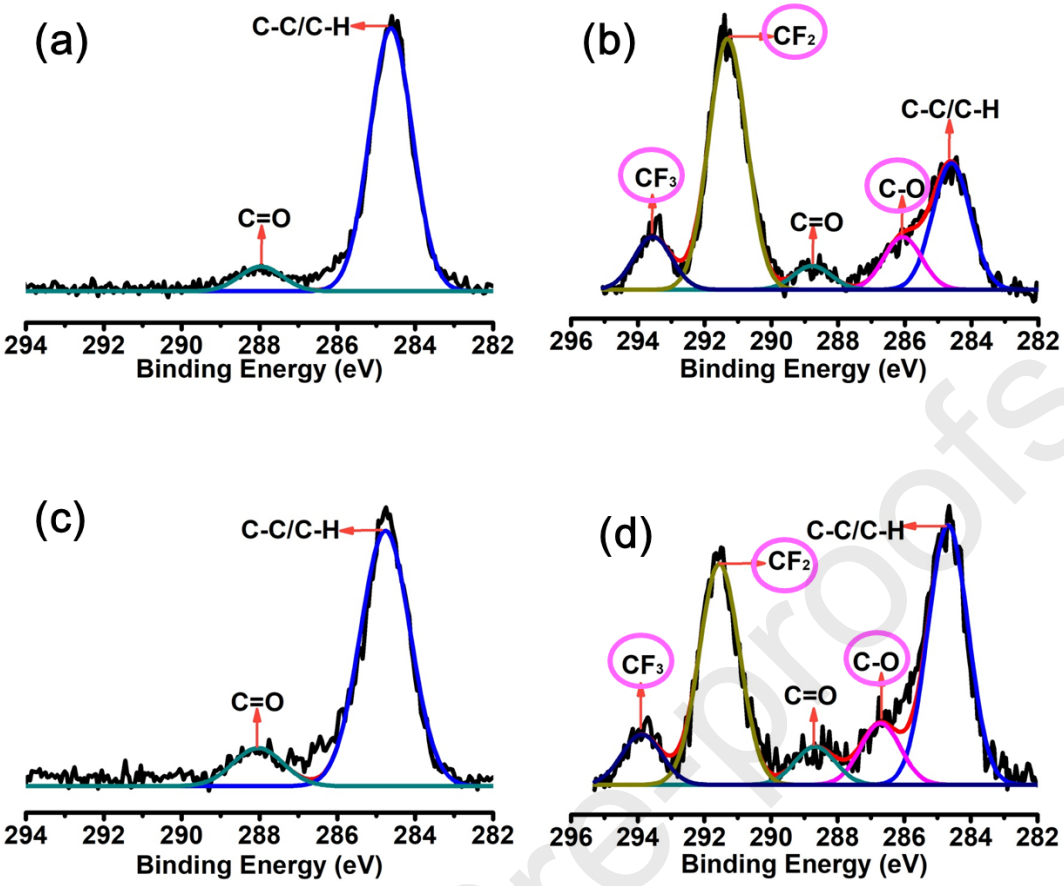

Fig. 5. High-resolution C1s XPS spectra and their peak fitting curves of the samples (a) NS, (b) NSF, (c) DS, and (d) DSF.

The surface wettability of the as-prepared samples was examined to clarify the correlation between the surface topography, chemistry and hydrophobic performances. The water CA values of flat silicon wafers before and after the fluorination treatment are about 59° and 108° respectively (**Fig. S4**). Prior to surface hydrophobicity, both of the NS and DS surfaces exhibit unmeasurably low CAs. In a sharp contrast, all the fluorinated samples display ultrahigh static CA values, whereas some obvious differences are also observed. As for the single-scale surface, the NSF (161.3 °) is more hydrophobic than MSF (151.1°), but the CA value is relatively lower than that on the DSF (174.0°) (**Fig. 6a-c**). The reason is that the dual-scale structured surface can capture more air at the interfaces between water and solid so as to achieve a more stable Cassie-Baxter wetting regime [44-46]. On the other hand, more prominent differences in dynamic roll-off angle (RA) were observed among the samples. The

RA values of NSF and MSF are 6.3° and 27.4° respectively, presumably due to the different metastable positions of heterogeneously wetting as illustrated by the modal pictures (**Fig. 6a(VI),b(IV)**) [47,48]. As for the DSF, water droplets (6 μL) can readily roll off the surface even with an extremely low tilted angle (RA < 1°), exhibiting a more distinguished water super-repellency.

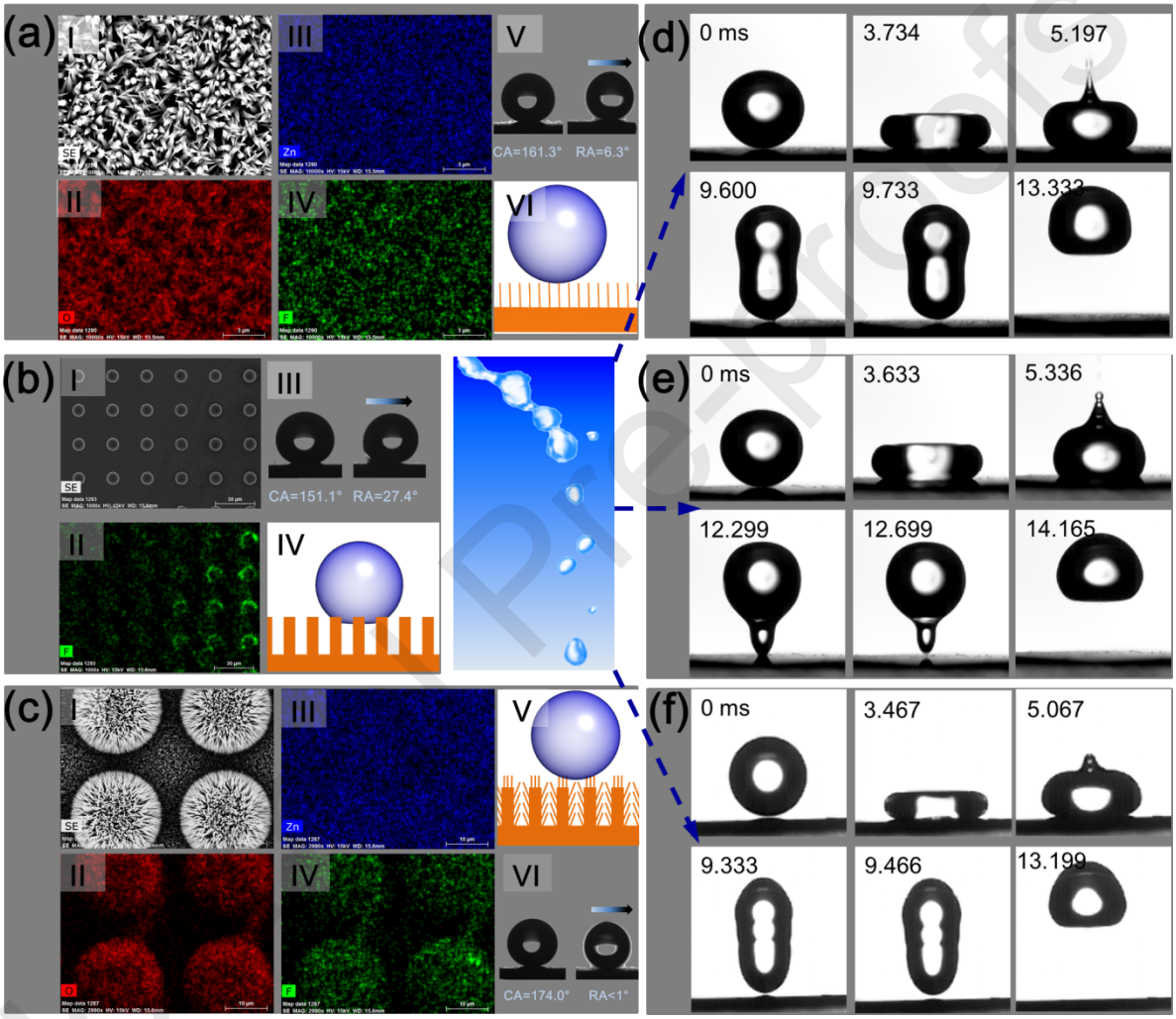

Fig. 6. Surface components and property of artificial structures. (a-c) SEM image at top view, the distribution of O (red), Zn (dark blue) and F (green) elements, the CA, RA and schematic states of Cassie–Baxter of the NSF (a), MSF (b), DSF (c). (d-f) Droplets bouncing behaviors of surfaces NSF (d), MSF (e) and DSF (f).

The bouncing of droplets is another characteristic feature related to the dynamic wetting behavior, which can indirectly reflect the adhesive property between a water droplet and a

surface [49,50]. When a droplet impacts a non-wetting surface, it will first reach a maximum diameter and then retract to certain extent before it completely rebounds and leaves the solid material [51]. To provide more insight into the water super-repellency, the water drop impact test was carried out by dropping a 6 μL water droplet from a height of 80 mm above the surface, which was recorded by a high-speed camera at the rate of 6000 frames s^{-1} (**Fig. 6d-f**). As a crucial criterion to quantify the surface water-repellent performance, water-surface "contact time", defined as the amount of time that the drop is in contact with the solid during the drop impacting process [49,51], was explored. For consistency, the initial contact time is defined as the time at which only a small part of the droplet touched the surface and the droplet still maintained a spherical shape approximately. Among those samples, the MSF surface presents the longest contact time of ~12.699 ms. It can be interpreted that dripping droplets can extrude more air from the MSF surface and increase the contact area between the liquid and solid surface, causing an obvious delay in its rebounding time [52]. In contrast, much shorter rebound time of water droplets is needed on the surfaces of both the NSF and the DSF. Interestingly, the rebound time on the NSF surface (9.733 ms) is nearly comparable to that on the DSF (9.466 ms), despite of a big structural difference between the single-scale NSF and the dual-scale DSF. Therefore, we believe that the outermost nano-needles play a more vital role in water droplet rebounding than their hierarchical structures. Both NSF and DSF surfaces show a straightforward detaching behavior, whereas the MSF surface exerts a "reluctant" detaching process with an obvious "tail" at the bottom of the drop. These results indirectly demonstrate that the DSF and the NSF surfaces are more efficient in repelling the impacting water than the MSF surface and getting liquid free surfaces.

3.4 Biomimetic surface antibacterial properties

Till now, most previous bactericidal surfaces based on physical structures have focused on exploring the lethal mechanism, optimizing the killing efficiency and simplifying the manufacture processes [5,6,14,53], whereas with very few attentions on the long-term

antibacterial performances. Encouraged by the synergistic antibacterial effects of lotus leaf surface, the super-repellency and mechanical bactericidal property of the as-prepared samples are also highly desired. Similarly, to evaluate the antibacterial capabilities, all the samples (0.5 × 0.5 cm^2) were immersed in 2 mL *E. coli* suspensions (~10^8 CFU mL^{-1}, PBS) for 3, 6, 12, and 24 h incubation, respectively.

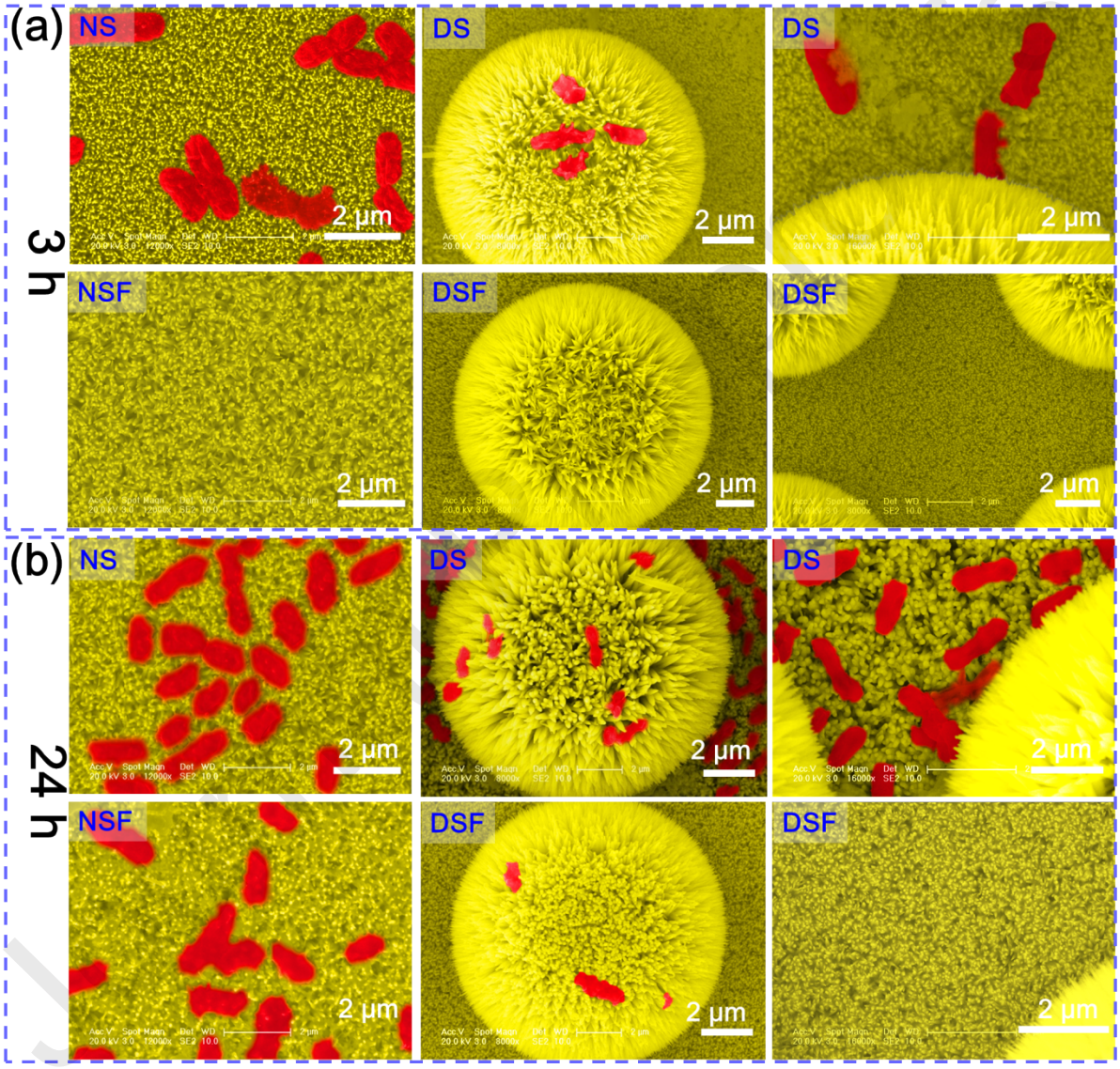

Fig. 7. Representative SEM images of *E. coli* cells morphologies adhered on the samples after 3 h (a), and 24 h (b) incubation.

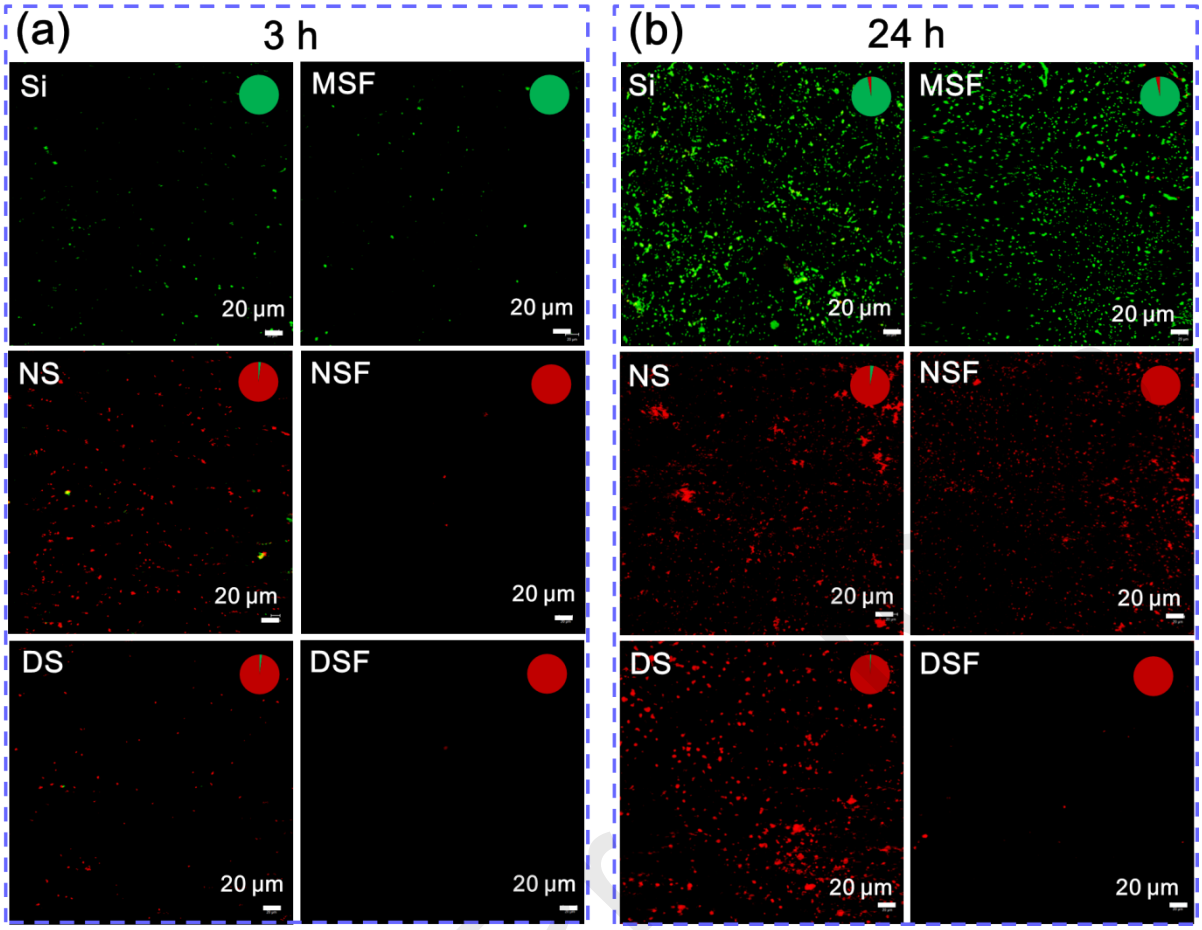

Fig. 8. CLSM images of bacteria attached on the ZnO nanoneedles modified surfaces after 3 h (c) and 24 h (d) incubation; the red spots indicate the non-viable bacterial cells, whereas the living cells were stained as green. Corresponding percentages of live (green) and dead (red) bacteria are plotted in the top right corner of the images.

The bactericidal capability and mechanism were firstly studied. As shown in **Fig. 7a,b,** the bacterial cells attached on all of the ZnO nanoneedles modified surfaces present strongly deformed morphologies with shrunken, empty, and engulfed appearances, similar to that on the lotus leaf and other mechanical bactericidal surfaces [6]. In contrast, the majority of attached bacteria on the planar silicon wafer and MSF surfaces keep intact cell morphology with native rod shape which is a typical identification of live bacteria **(Fig. S5)**. CLSM images further confirmed these results. On the surfaces without modification of ZnO nanopillars, most bacteria cells are stained green (activated state), on the other hand, the

bacteria on the ZnO nanoneedle coated surfaces display dead state (marked red color) (**Fig. 8 and Fig. S6**). Intriguingly, despite the significant difference in surface chemistry and wettability, all ZnO nanoneedle coated surfaces (NS, DS, NSF and DSF) present strong bactericidal activities that more than 98% of bactericidal efficiency can be achieved over the full incubating time (bactericidal efficiency = red coverage/(the total area of red and green coverages)). Thus the death of attached bacteria can be ascribed purely to the nanoneedles rather than the chemical composition of the surface. This is consistent with previous report that, as for the mechanical bactericidal surfaces, the surface chemistry properties scarcely influence the sterilizing effectiveness [6,15].

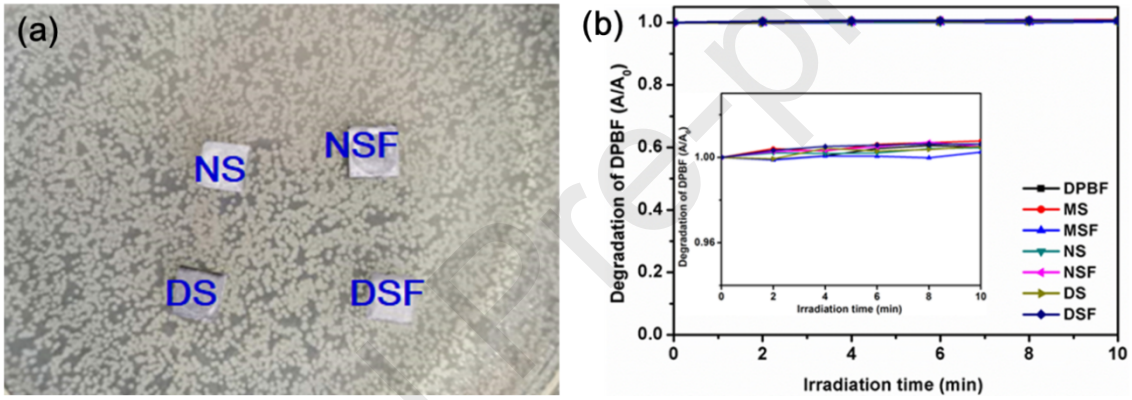

Fig. 9. (a) Digital images of the inhibition zones of samples against *E. coli*. (b) Time-dependent UV-vis spectrum of DPBF under the illumination of the UV (30 W, λ = 365 nm) after irradiation from 0 to 10 min. Inset in (b): magnified views in the vertical scale.

To determine whether the zinc ions detach from the ZnO nanoneedles and affect the lethality against *E. coli*, zone inhibition assay was carried out. As shown in **Fig. 9a**, no obvious inhibition zone is observed around all of the samples, indicating no essential bactericidal activity deriving from the released zinc ions. As reported, the reactive oxygen species (ROS) could be harmful to the cell wall and even kill the contacted bacteria [15]. To explore the influence of ROS generated by the samples, the amounts of generated ROS were essentially detected using 1,3-diphenylisobenzofuran (DPBF) as a chemical probe under ambient light. As shown in **Fig. 9b**, there is no obviously detectable amount of ROS for all

samples, eliminating the detrimental effect of ROS in this system. These results clearly indicate the bactericidal performances of the nanoneedles patterned surfaces can be exclusively attributed to the physical structures.

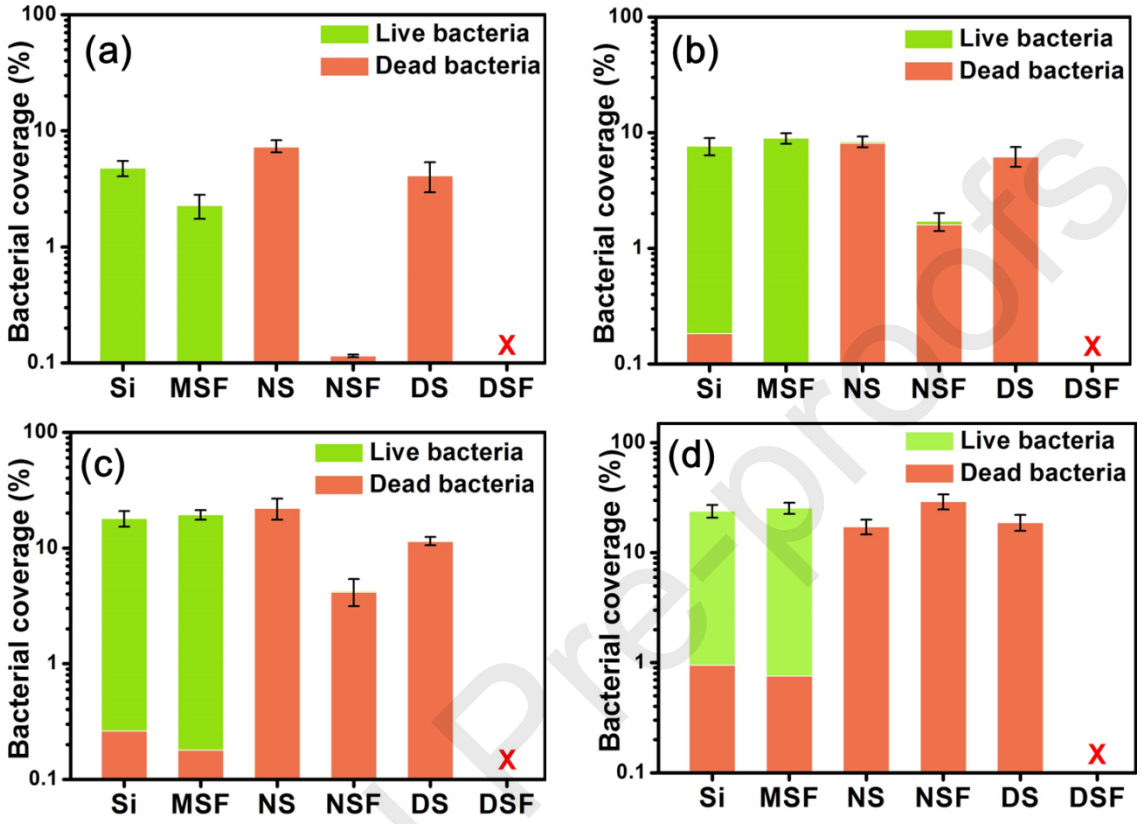

Fig. 10. The corresponding bacterial coverage statistics of CLSM images after 3 h (a), 6 h (b), 12 h (c) and 24 h (d) incubation intervals.

Although the above results demonstrate that all of ZnO nanoneedles coated surfaces present strong bactericidal activities, generally, sole mechanical bactericidal surfaces usually suffer from the accumulation of dead bacteria and debris, which can largely shield the functionalized structures, thereby remarkably reducing the surface bactericidal activity. Therefore, to realize a long-term antibacterial efficacy, it is crucial for mechanical bactericidal surfaces possessing an excellent super-repellency to prevent most of the initial bacterial adhesion, simultaneously [53]. In this regard, the bacterial repellency (or non-fouling property) of the as-prepared surfaces was further investigated. As shown in **Fig. 10a and S6a**, almost no any bacterial adhesion is found on the superhydrophobic NSF and DSF surfaces after the initial 3 h

incubation. This excellent antibacterial performance is attributed to the existence of the steady air cushion at the interface of the superhydrophobic surface and the bacterial suspension, which defends the surface from being contaminated by bacteria [38]. On the other hand, though the MSF surface displays some superhydrophobic characteristics, a very limited reduction (~39.1%) in bacterial adhesion is observed, as compared to those on the control silicon wafer. This result is in accord with the previous report that the superhydrophobic cicada wing even enabled bacterial cell adhesion [6], as explained by the fact that the Wenzel regime superhydrophobic surfaces may fail to markedly minimize the essential water/solid interfacial contact area and effectively prevent bacterial adhesion owing to the lack of the stable air obstacle [34]. Prolonging the incubation time leads to obvious reductions for their bacterial super-repellency. After 12 h exposure to the bacterial medium, the NSF surface displays an obvious increase in bacterial coverage, evidently indicating the abated bacterial repellency (**Fig. 10c and S6c**). As shown in **Fig.10a,d,** the number of bacteria adhered on the NSF increases up to ~140-fold after 24 h incubation compared to its counterpart with 3 h, which are even higher than that on the NS after 24 h exposure. In contrast, the DSF demonstrates excellent bacterial repellent performances regardless the incubation time, more than 99% reduction in bacterial adhesion is achieved on the surface after 24 h incubation, with respect to the control silicon wafer. This bacterial super-repellency is mainly attributed to the stable superhydrophobic Cassie-Baxter state of the DSF surface that can remarkably minimize the liquid/solid interfacial contact area and reduce the bacterial adhesion.

Interestingly, the few adhered bacteria on the DSF only locate on the peak of the hierarchical papillae and no any cells are found on the valley (between the micro-papillae) (**Fig. 7b (DSF)**). On the contrary, as for the superhydrophilic DS surface (WCA $\leq 5^{o}$), more bacteria adhere on the valley rather than the peak (**Fig. 7b (DS)**). This inconsistency is likely due to the interfacial wetting differences between the superhydrophobic DSF and the superhydrophilic DS, as illustrated in **Fig. 11a,b**. Owing to the good surface wettability of the

DS, the bacterial adhesion is predominantly governed by its surface topological structures, which prefers to the edge of the papillae rather than the top part [54-56]. On the other hand, because of the existed air cushion in the interfaces between medium and the DSF surface, the valley parts of the DSF structures are immune to the bacterial contamination, so that only few bacteria have the chance to contact with the top part of the papillae. More importantly, as shown in the **Fig. 7b (DSF) and 8b (DSF)**, the few attached bacteria can be effectively killed by nanoneedles. The DSF surface presents both of remarkable bacterial super-repellency and significantly mechanical bactericidal efficiency. Therefore, this DSF surface based on synergistic antibacterial performances can significantly prolong its antibacterial efficiency with respect to the surfaces with sole superhydrophobic or physical bactericidal properties.

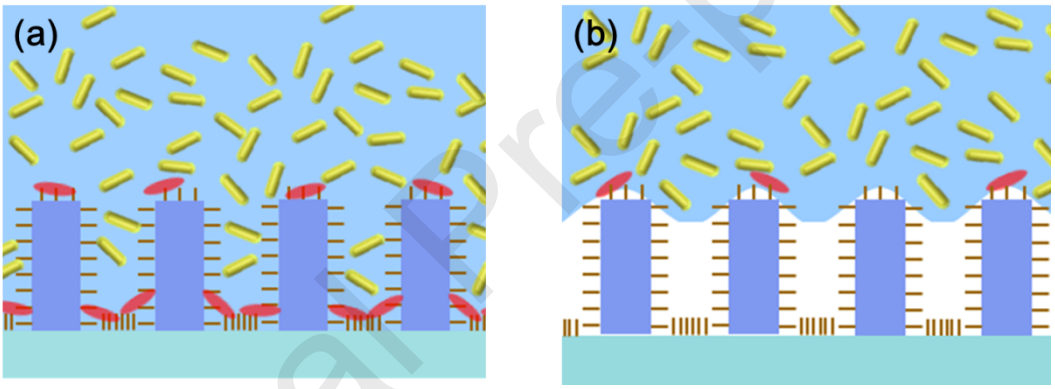

Fig. 11. Schematic of the bacterial medium interacts with DS (a) and DSF (b) surfaces (yellow rods represent live cells and red rods represent dead cells).

3.5 Antibacterial recycle assay

A recyclable antibacterial surface with no obviously compromised efficiency is also highly desired for certain clinical applications [57]. Up to now, to the best of our knowledge, such a mechanical bactericidal surface with recyclable functionalities has not been reported. Given the extraordinary stability and prominent antibacterial properties of DSF surface, its antibacterial activity after four cycles was examined. For each recycle, the samples were incubated in 2 mL bacterial suspension (~10^8 CFU mL^{-1}, PBS) at 37 °C for 12 h, subsequently rinsed with sterile PBS for three times and dried in air for 30 min. The

suspension was replaced every 6 h to maintain the bacterial cell vitality. Similar to most conventional mechanical bactericidal surfaces, just undergoing one single cycle, the NS and DS surfaces are readily covered by dead cells, and more serious bacterial adhesions, including both live and dead cells, were observed after 4-cycle bacterial contamination (**Fig. 12 and Fig. 13**). A few of dead bacteria are observed on the superhydrophobic NSF surface after undergoing the first cycle. Increasing the contamination process leads to a steady and prominent increase in bacterial adhesion on NSF, and a ~37% bacterial coverage with large number of live bacteria (green spots) is observed after being treated by a 4-cycle contamination. These phenomena indicate that the incompetent bacterial repellency could lead to the failure of mechanical bactericidal performance due to the accumulated dead bacteria and debris after repeated or long-term bacterial contaminations. In stark contrast, even going through four cycles of bacterial contamination, the DSF surface still remains robust bacterial super-repellency and remarkable mechanical bactericidal performance, which repels most of the bacteria and readily kills all the adhered residuals getting a totally bacteria-free surface (**Fig. 12d and Fig. 13**). These results also demonstrate that this synergistic antibacterial surface, DSF, can maintain a cleaning surface and effective mechano-killing properties even suffering from repeated bacterial contaminations which provides great potential in reusable surgical devices.

Journal Pre-proofs

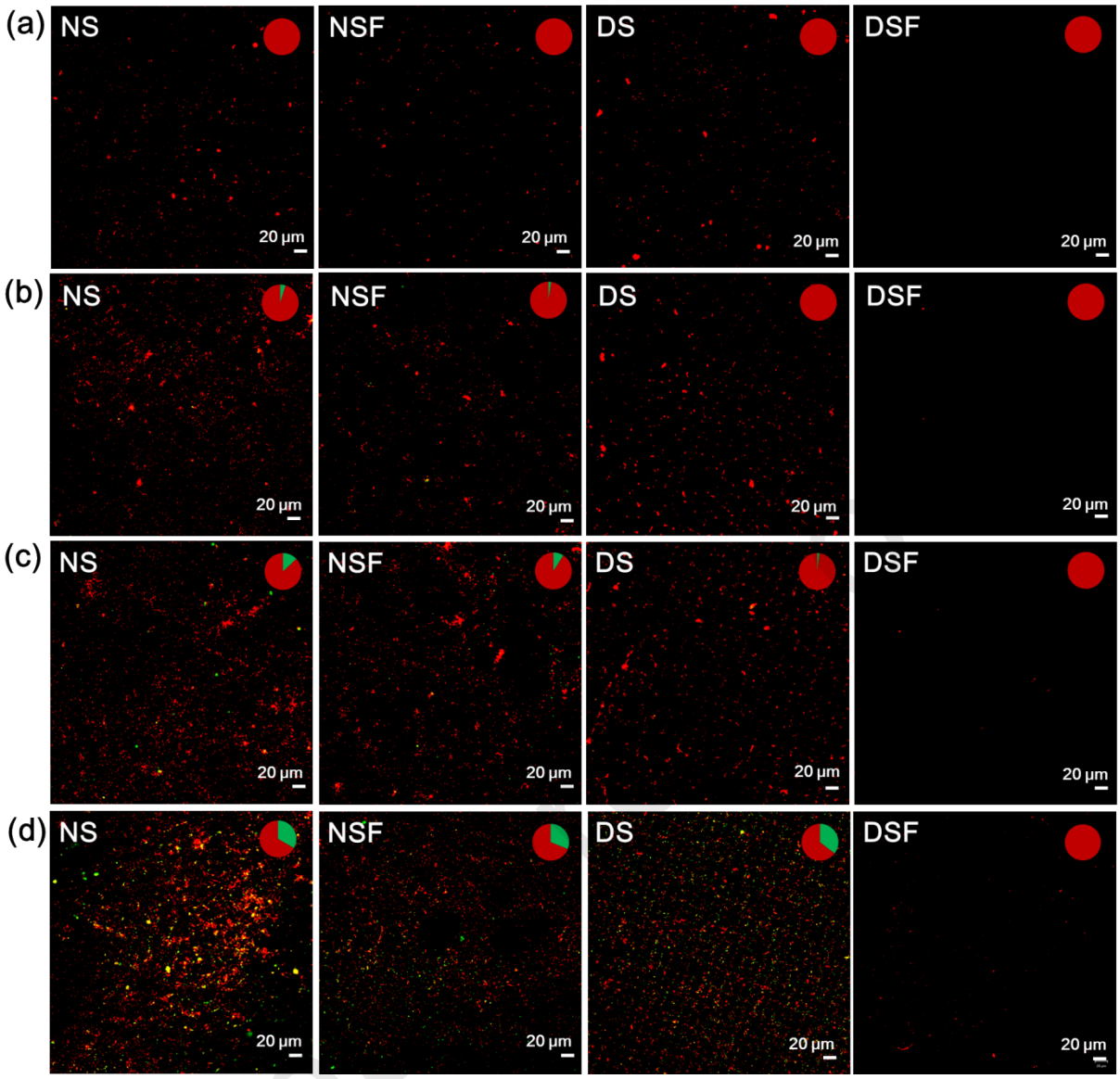

Fig. 12. Representative CLSM images of *E. coli* cells attachment to samples after four cycles of incubation. (a-d) CLSM images of the bacterial coverage after one (a), two (b), three (c), and four (d) cycles of bacterial contamination. Green and red spots represent live and non-viable bacterial cells respectively. Corresponding percentages of live (green) and dead (red) bacteria are plotted in the top right corner of the images.

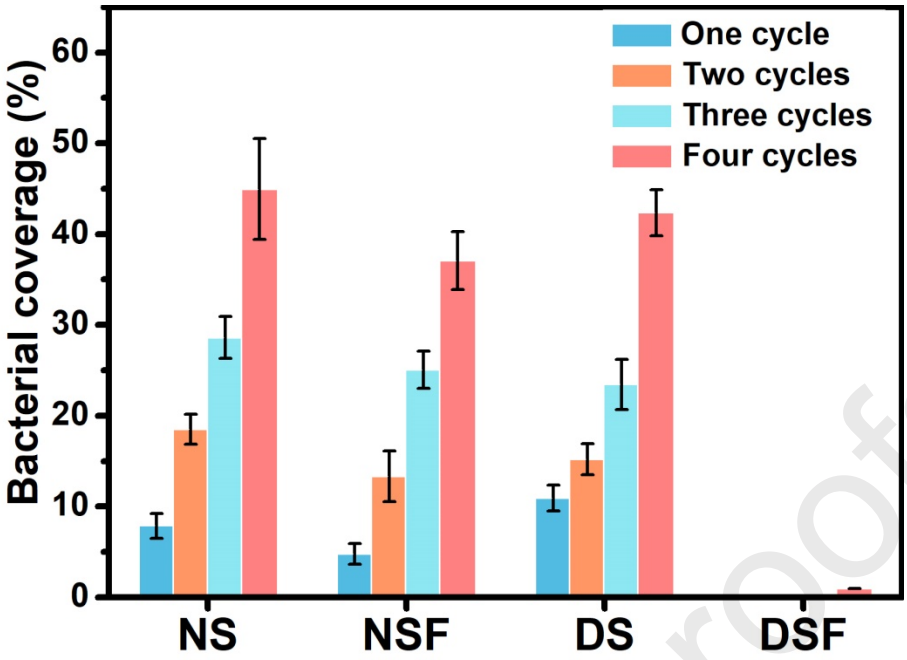

Fig. 13. The corresponding bacterial coverage statistics of CLSM images after various cycles of incubation.

4. Conclusions

In summary, we have found that the hierarchical structures of the natural lotus leaf maintain synergistic antibacterial properties, involving both the remarkable bacterial super-repellency (non-fouling property) in the initial stage and effective bactericidal activity against adhered *E. coli*. Further investigations illustrate that the death of the bacteria is purely caused by their physical structure through a cell-rupturing mechanism. Inspired by this, we successfully develop a lotus-leaf-alike superhydrophobic surface with ultra-high contact angle (>174°) and extremely low roll-off angle (<1°) *via* a combined method of plasma etching and low-temperature hydrothermal reaction. Compared to regular superhydrophobic (non-fouling to some extent, but no bacteria-killing) or mechanical bactericidal surfaces (bacteria-killing but not bacteria-repelling), this biomimetic surface displays more advanced synergistic antibacterial performances, with long-term bacterial super-repellency, effective and durable mechanical bactericidal activity. Moreover, this biomimetic surface even goes through four cycles bacterial contamination can get a surface with no viable bacteria. Benefiting from the

bio-inspired synergistic strategy derived from the pure physical phenomena, this biomimetic surface shows great potentials as an excellent antibacterial platform without causing risks of AMR. Additionally, the discoveries of the lotus leaf which could inactivate bacteria depending on its random arranged tubes may extend our inspiration in exploring the mechanical bactericidal structures. In next works, the dimensions of the hierarchical structures will be varied to explore their influences to different types of microorganisms.

Declaration of Competing Interest

The authors declare no conflict of interest.

Acknowledgements

The authors gratefully acknowledge the financial support through the National Science Foundation of China (No. 51775232, 51803212, 51875240), the Science and Technology Development Plan Project of Jilin Province (No. 20190201155JC) and the Fundamental Research Funds for the Central Universities.

References

[1] M. Tyers, G. D. Wright, Drug combinations: a strategy to extend the life of antibiotics in the 21st century, Nat. Rev. Microbiol. 17 (2019) 141-155.

[2] M. Baym, L. K. Stone, R. Kishony, Multidrug evolutionary strategies to reverse antibiotic resistance, Science 351 (2016) 40-46.

[3] World Health Organization: Global priority list of antibiotic-resistant bacteria to guide research, discovery, and development of new antibiotics. (2017) http://www.who.int/medicines/publications/.

[4] U. Theuretzbacher, Global antimicrobial resistance in Gram-negative pathogens and clinical need. Curr. Opin. Microbiol. 39 (2017) 106-112.

[5] E. P. Ivanova, J. Hasan, H. K. Webb, V. K. Truong, G. S. Watson, J. A. Watson, V. A. Baulin, S. Pogodin, J. Y. Wang, M. J. Tobin, C. Lobbe, R. J. Crawford, Natural

Journal Pre-proofs

bactericidal surfaces: mechanical rupture of Pseudomonas aeruginosa cells by cicada wings, Small 8 (2012) 2489-2494.

[6] E. P. Ivanova, J. Hasan, H. K. Webb, G. Gervinskas, S. Juodkazis, V. K. Truong, A. H. Wu, R. N. Lamb, V. A. Baulin, G. S. Watson, J. A. Watson, D. E. Mainwaring, R. J. Crawford, Bactericidal activity of black silicon, Nat. Commun. 4 (2013) 2838.

[7] D. E. Mainwaring, S. H. Nguyen, H. Webb, T. Jakubov, M. Tobin, R. N. Lamb, A. H.-F. Wu, R. Marchant, R. J. Crawford, E. P. Ivanova, The nature of inherent bactericidal activity: insights from the nanotopology of three species of dragonfly, Nanoscale 8 (2016) 6527-6534.

[8] S. Kim, U. T. Jung, S. K. Kim, J. H. Lee, H. S. Choi, C. S. Kim, M. Y. Jeong, Nanostructured multifunctional surface with antireflective and antimicrobial characteristics, ACS Appl. Mater. Interfaces 7 (2015) 326-331.

[9] S. Wu, F. Zuber, J. Brugger, K. Maniura-Weber, Q. Ren, Antibacterial Au nanostructured surfaces, Nanoscale 8 (2016) 2620-2625.

[10] Tripathy, S. Pahal, R. J. Mudakavi, A. M. Raichur, M. M. Varma, P. Sen, Impact of bioinspired nanotopography on the antibacterial and antibiofilm efficacy of chitosan, Biomacromolecules 19 (2018) 1340-1346.

[11] G. S. Watson, D. W. Green, L. Schwarzkopf, X. Li, B. W. Cribb, S. Myhra, J. A. Watson, A gecko skin micro/nano structure-A low adhesion, superhydrophobic, anti-wetting, self-cleaning, biocompatible, antibacterial surface, Acta. Biomater. 21 (2015) 109-122.

[12] C. D. Bandara, S. Singh, I. O. Afara, A. Wolff, T. Tesfamichael, K. Ostrikov, A. Oloyede, Bactericidal effects of natural nanotopography of dragonfly wing on Escherichia coli, ACS Appl. Mater. Interfaces 9 (2017) 6746-6760.

[13] G. S. Watson, D. W. Green, B. W. Cribb, C. L. Brown, C. R. Meritt, M. J. Tobin, J. Vongsvivut, M. Sun, A. P. Liang, J. A. Watson, Insect analogue to the lotus leaf: A planthopper wing membrane incorporating a low-adhesion, nonwetting, superhydrophobic,

Journal Pre-proofs

bactericidal, and biocompatible surface, ACS Appl. Mater. Interfaces 9 (2017) 24381-24392.

[14] D. P. Linklater, M. De Volder, V. A. Baulin, M. Werner, S. Jessl, M. Golozar, L. Maggini, S. Rubanov, E. Hanssen, S. Juodkazis, E. P. Ivanova, High aspect ratio nanostructures kill bacteria via storage and release of mechanical energy, ACS nano 12 (2018) 6657-6667.

[15] G. Yi, Y. Yuan, X. Li, Y. Zhang, ZnO Nanopillar Coated Surfaces with Substrate-Dependent Superbactericidal Property, Small 14 (2018) 1703159.

[16] Tripathy, P. Sen, B. Su, W. H. Briscoe, Natural and bioinspired nanostructured bactericidal surfaces, Adv. Colloid Interface Sci. 248 (2017) 85-104.

[17] K. Modaresifar, S. Azizian, M. Ganjian, L. E. Fratila-Apachitei, A. A. Zadpoor, Bactericidal effects of nanopatterns: A systematic review, Acta. Biomater. 83 (2019) 29-36.

[18] Elbourne, J. Chapman, A. Gelmi, D. Cozzolino, R. J. Crawford, V. K. Truong, Bacterial-nanostructure interactions: The role of cell elasticity and adhesion forces, J. Colloid Interface Sci. 546 (2019) 192-210.

[19] D. P. Linklater, H. K. D. Nguyen, C. M. Bhadra, S. Juodkazis, E. P. Ivanova, Nanofabrication of mechano-bactericidal surfaces, Nanoscale 9 (2017) 16564-16585.

[20] S. Pogodin, J. Hasan, V. A. Baulin, H. K. Webb, V. K. Truong, T. H. Phong Nguyen, V. Boshkovikj, C. J. Fluke, G. S. Watson, J. A. Watson, R. J. Crawford, Biophysical model of bacterial cell interactions with nanopatterned cicada wing surfaces, E. P. Ivanova, Biophys. J. 104 (2013) 835-840.

[21] C. M. Bhadra, M. Werner, V. A. Baulin, V. K. Truong, M. Al Kobaisi, S. H. Nguyen, A. Balcytis, S. Juodkazis, J. Y. Wang, D. E. Mainwaring, Subtle variations in surface properties of black silicon surfaces influence the degree of bactericidal efficiency, Nano-Micro Lett. 10 (2018) 36.

[22] D. H. Nguyen, C. Loebbe, D. P. Linklater, X. Xu, N. Vrancken, T. Katkus, S. Juodkazis, S. Maclaughlin, V. Baulin, R. J. Crawford, The idiosyncratic self-cleaning cycle of bacteria

Journal Pre-proofs

on regularly arrayed mechano-bactericidal nanostructures, Nanoscale 11 (2019) 16455-16462.

[23] T. Wei, Z. Tang, Q. Yu, H. Chen, Smart antibacterial surfaces with switchable bacteria-killing and bacteria-releasing capabilities, ACS Appl. Mater. Interfaces 9 (2017) 37511-37523.

[24] P. Zhang, L. Lin, D. Zang, X. Guo, M. Liu, Designing Bioinspired Anti-Biofouling Surfaces based on a Superwettability Strategy, Small 13 (2017) 1503334.

[25] T. Darmanin, F. Guittard, Superhydrophobic and superoleophobic properties in nature, Mater. Today 18 (2015) 273-285.

[26] T. Darmanin,F. Guittard, Recent advances in the potential applications of bioinspired superhydrophobic materials, J. Mater. Chem. A 2 (2014) 16319-16359.

[27] K. Liu, X. Yao, L. Jiang, Recent developments in bio-inspired special wettability, Chem. Soc. Rev. 39 (2010) 3240-3255.

[28] K. Koch, B. Bhushan, Y. C. Jung, W. Barthlott, Fabrication of artificial Lotus leaves and significance of hierarchical structure for superhydrophobicity and low adhesion, Soft Matter. 5 (2009) 1386.

[29] K. Koch, B. Bhushan, W. Barthlott, Multifunctional surface structures of plants: An inspiration for biomimetics, Prog. Mater. Sci. 54 (2009) 137-178.

[30] W. Barthlott, C. Neinhuis, Purity of the sacred lotus, or escape from contamination in biological surfaces, Planta 202 (1997) 1-8.

[31] J. Zhao, L. Song, J. Yin, W. Ming, Anti-bioadhesion on hierarchically structured, superhydrophobic surfaces, Chem. Commun. 49 (2013) 9191-9193.

[32] C. Schlaich, M. Li, C. Cheng, I. S. Donskyi, L. Yu, G. Song, E. Osorio, Q. Wei, R. Haag, Mussel-Inspired Polymer-Based Universal Spray Coating for Surface Modification: Fast Fabrication of Antibacterial and Superhydrophobic Surface Coatings, Adv. Mater. Interfaces 5 (2018) 1701254.

Journal Pre-proofs

[33] W. Wang, Y. Lu, H. Zhu,Z. Cao, Superdurable Coating Fabricated from a Double-Sided Tape with Long Term "Zero" Bacterial Adhesion, Adv. Mater. 29 (2017) 1606506.

[34] X. Zhang, L. Wang, E. Levänen, Superhydrophobic surfaces for the reduction of bacterial adhesion, RSC Adv. 3 (2013) 12003.

[35] B. J. Privett, J. Youn, S. A. Hong, J. Lee, J. Han, J. H. Shin, M. H. Schoenfisch, Antibacterial fluorinated silica colloid superhydrophobic surfaces, Langmuir 27 (2011) 9597-9601.

[36] M. Zhang, P. Wang, H. Sun, Z. Wang, Superhydrophobic surface with hierarchical architecture and bimetallic composition for enhanced antibacterial activity, ACS Appl. Mater. Interfaces 6 (2014) 22108-22115.

[37] B. Bhushan,Y. C. Jung, Natural and biomimetic artificial surfaces for superhydrophobicity, self-cleaning, low adhesion, and drag reduction, Prog. Mater. Sci. 56 (2011) 1-108.

[38] G. B. Hwang, K. Page, A. Patir, S. P. Nair, E. Allan, I. P. Parkin, The anti-biofouling properties of superhydrophobic surfaces are short-lived, ACS nano 12 (2018) 6050-6058.

[39] H. V. Jansen, M. J. de Boer, S. Unnikrishnan, M. C. Louwerse, M. C. Elwenspoek, Black silicon method X: a review on high speed and selective plasma etching of silicon with profile control: an in-depth comparison between Bosch and cryostat DRIE processes as a roadmap to next generation equipment, J. Micromech. Microeng. 19 (2009) 033001.

[40] Y. Hou, M. Yu, X. Chen, Z. Wang, S. Yao, Recurrent filmwise and dropwise condensation on a beetle mimetic surface, ACS nano 9 (2014) 71-81.

[41] Z. Han, X. Feng, Z. Guo, S. Niu, L. Ren, Flourishing bioinspired antifogging materials with superwettability: progresses and challenges, Adv. Mater. 30 (2018) 1704652.

[42] J. Tian, J. Zhu, H. Y. Guo, J. Li, X. Q. Feng, X. Gao, Efficient self-propelling of small-scale condensed microdrops by closely packed ZnO nanoneedles, J. Phys. Chem. Lett. 5 (2014) 2084-2088.

[43] M. Michalska, F. Gambacorta, R. Divan, I. S. Aranson, A. Sokolov, P. Noirot, P. D. Laible, Tuning antimicrobial properties of biomimetic nanopatterned surfaces, Nanoscale 10 (2018) 6639-6650.

[44] K. Kota, Y. Li, J. M. Mabry, A. Tuteja, Hierarchically structured superoleophobic surfaces with ultralow contact angle hysteresis, Adv. Mater. 24 (2012) 5838-5843.

[45] E. Bittoun, A. Marmur, The role of multiscale roughness in the lotus effect: is it essential for super-hydrophobicity? Langmuir 28 (2012) 13933-13942.

[46] C. R. Szczepanski, F. Guittard, T. Darmanin, Recent advances in the study and design of parahydrophobic surfaces: From natural examples to synthetic approaches, Adv. Colloid Interface Sci. 241 (2017) 37-61.

[47] S. Wang, K. Liu, X. Yao, L. Jiang, Bioinspired Surfaces with Superwettability: New Insight on Theory, Design, and Applications, Chem. Rev. 115 (2015) 8230-8293.

[48] K. Liu, Y. Tian, L. Jiang, Bio-inspired superoleophobic and smart materials: Design, fabrication, and application, Prog. Mater. Sci. 58 (2013) 503-564.

[49] D. Richard, C. Clanet, D. Quéré, Surface phenomena: Contact time of a bouncing drop, Nature 417 (2002) 811.

[50] B. Zhang, Q. Lei, Z. Wang, X. Zhang, Droplets can rebound toward both directions on textured surfaces with a wettability gradient, Langmuir 32 (2015) 346-351.

[51] J. C. Bird, R. Dhiman, H.-M. Kwon, K. K. Varanasi, Reducing the contact time of a bouncing drop, Nature 503 (2013) 385.

[52] P. Tsai, S. Pacheco, C. Pirat, L. Lefferts, D. Lohse, Drop impact upon micro-and nanostructured superhydrophobic surfaces, Langmuir 25 (2009) 12293-12298.

[53] N. Rauner, C. Mueller, S. Ring, S. Boehle, A. Strassburg, C. Schoeneweiss, M. Wasner, J. C. Tiller, A Coating that Combines Lotus-Effect and Contact-Active Antimicrobial Properties on Silicone, Adv. Funct. Mater. 28 (2018) 1801248.

[54] J. Ma, Y. Sun, K. Gleichauf, J. Lou, Q. Li, Nanostructure on taro leaves resists fouling by colloids and bacteria under submerged conditions, Langmuir 27 (2011) 10035-10040.

[55] H. Gu, A. Chen, X. Song, M. E. Brasch, J. H. Henderson, D. Ren, How Escherichia coli lands and forms cell clusters on a surface: a new role of surface topography, Sci. Rep. 6 (2016) 29516.

[56] F. Song, H. Koo, D. Ren, Effects of material properties on bacterial adhesion and biofilm formation, J. Dent. Res. 94 (2015) 1027-1034.

[57] S. Yan, H. Shi, L. Song, X. Wang, L. Liu, S. Luan, Y. Yang, J. Yin, Nonleaching bacteria-responsive antibacterial surface based on a unique hierarchical architecture, ACS Appl. Mater. Interfaces 8 (2016) 24471-24481.

Highlights

- The lotus leaf demonstrated not only repellency against bacteria but bactericidal activity.
- The bactericidal mechanism has been proved to be a cell-rupturing effect.
- A hierarchically structured surface was designed and prepared.
- The artificial surface displayed synergistic antimicrobial activity based entirely on physical mechanism.
- The structured surface has the great advantage in maintaining long-term effectiveness in antimicrobial activity.

Journal Pre-proofs